PHYSICAL REVIEW A VOLUME 49, NUMBER 5 MAY 1994

Broadening and shifts of the lines of molecular ions by collisions with neutral perturbers

G. Buffa and O. Tarrini
Dipartimento di Fisica dell'Università, Piazza Torricelli 2, I-56126 Pisa, Italy

G. Cazzoli and L. Dore
Dipartimento di Chimica dell'Università, Via Selmi 2, I-40126 Bologna, Italy

(Received 30 July 1993)

We present a theoretical model for studying the shape of the rotational lines of molecular ions perturbed by collisions with neutral species. This model shows that the interaction between the ionic monopole and the multipole moments of the perturber has no role in the collisional relaxation of the lines. The effect of the ionic monopole is restricted to that of inducing a polarization of the neutral perturbers that can cause relaxation by interaction with the other permanent moments of the absorbing ion. We also present, for HCO^+ perturbed by argon, an experimental study of the pressure broadening and shift of the rotational lines $J = 1 \leftarrow 0$, $2 \leftarrow 1$, and $4 \leftarrow 3$. The agreement between theory and experiment is satisfactory.

PACS number(s): 33.70.Jg, 33.20.Bx

I. INTRODUCTION

The collisional broadening of the rotational spectral lines of neutral molecules has recently received much attention both experimentally and theoretically. By contrast, the broadening of the spectra of molecular ions due to collisions with neutral perturbers is less well investigated, in spite of its interest and importance, particularly in the interpretation of radio astronomical data.

In the absence of measured or calculated values, estimates [1, 2] of linewidths 20 or 30 times as large as those for similar neutral molecules have been proposed. Such a large collisional broadening effect would prevent the observation of the rotational spectra of molecular ions. However, the observation of this kind of spectrum by Woods and co-workers [3] shows that the linewidths are comparable to those of similar neutrals or only slightly larger. This observation is supported by the semiclassical argument that the long range monopole force does not exert any torque on the ion. To date there has only been one study in the field, where the pressure broadening of the ion HCO^+ $J = 1 \leftarrow 0$ rotational transition by collision with several buffer gases was studied in a dc glow discharge [4].

In this paper we present an experimental study on HCO^+, produced in a magnetically enhanced negative glow, perturbed by argon. The collisional parameters were determined for three lines: $J = 1 \leftarrow 0$, $2 \leftarrow 1$, and $4 \leftarrow 3$. We also present a theoretical model for calculating both the pressure broadening and pressure shift coefficients for the spectral lines of ions perturbed by collisions with neutral species.

Our theoretical treatment shows that the interaction between the ionic monopole and the multipole moments, permanent or induced, of the perturber plays no role in the collisional relaxation. The effect of the ionic monopole is restricted to affecting the collisional trajectory and to inducing a polarization in the neutral perturber. The induced moments can produce relaxation by interaction with the permanent moments of the absorbing ion, with the exclusion of the monopole. In the case of HCO^+ perturbed by argon, by far the largest relaxation effect comes from the interaction between the dipole of the ion and the dipole induced in argon by the ionic charge.

Having clarified what interactions must be taken into account, we can extend to the case of ions the methods of calculation already used for neutral molecules. We give a detailed extension of the Anderson [5] -Tsao-Curnutte [6] (ATC) approximation for the dipole-monopole-induced dipole interaction, including also the pressure shift.

The experimental data show a decrease of pressure broadening parameters with increasing J, and show a change in sign of the pressure shift of the $J = 4 \leftarrow 3$ transition with respect to the lower J lines. The theoretical calculations confirm these results.

II. THEORY

In order to obtain the collisional broadening w and shift s of the spectral lines of an absorbing molecular ion interacting with neutral perturbers we follow the impact approximation [7].

We recall that in the frame of this theory, the relaxation terms w and s of a line $i \to f$ are linear in the number density n of the perturbing gas and can be expressed as the real and imaginary parts of a complex relaxation operator $\mathcal{R}$, averaged over all possible collisions:

$$w + is = n\langle \mathcal{R}(r,l)\rangle_{r,l}, \tag{1}$$

where $\langle\ \rangle_{r,l}$ represents the thermal average over the internal states r of the perturber and the angular momentum l of the relative motion.

1050-2947/94/49(5)/3557(9)/$06.00

The relaxation operator $\mathcal{R}$ can be derived from the scattering matrix S:

$$\mathcal{R}(r,l) = \mathbb{1} - \sum_{r'l'} \langle i,r,l|S|i,r',l'\rangle\langle f,r',l'|S^{\dagger}|f,r,l\rangle. \tag{2}$$

The scattering matrix S can be written in terms of the collisional interaction $V(t)$:

$$S = \mathcal{O}\exp\left(-\frac{1}{\hbar}\int_{-\infty}^{+\infty} dt\, e^{iH_0t/\hbar}V(t)e^{-iH_0t/\hbar}\right), \tag{3}$$

where H_0 is the unperturbed Hamiltonian of the two colliding partners and $\mathcal{O}$ is the time ordering operator.

From Eq. (3) we can see that if V is isotropic in the space of the internal degrees of the absorbing ion, then

$$\langle i,r,l|S|i,r',l'\rangle = \langle f,r,l|S|f,r',l'\rangle, \tag{4}$$

while

$$\langle i,r,l|S|i',r',l'\rangle = 0 \tag{5}$$

if the rotational state i' is different from i. Hence, Eq. (2) becomes

$$\mathcal{R}(r,l) = \mathbb{1} - \sum_{r'l'} |\langle i,r,l|S|i,r',l'\rangle|^2, \tag{6}$$

and by Eq. (5) and because of the unitary nature of S, $\mathcal{R}(r,l)=0$. Hence, we can conclude that the terms in V operating on the internal degrees of the absorbing ion by its monopole make no contribution to the relaxation of the line because they are isotropic.

Since an exact calculation of the scattering matrix is not easily made from Eq. (3) for anisotropic interactions, we resort to the semiclassical approximation [5, 6]. This assumes that the translational motion follows classical mechanics and uses quantum mechanics to describe the influence of the collision on the internal states of the molecules. Hence, Eq. (1) takes a form in which the translational state is described by the impact parameter b and the relative velocity v:

$$w + is = \left\langle 2\pi n v \int_0^{\infty} b\,db\,P(b,v,r)\right\rangle_{r,v}, \tag{7}$$

where we denote by P the semiclassical relaxation operator.

If the magnetic components are not resolved, the line $i, J_i \rightarrow f, J_f$ is in fact a superimposition of degenerate magnetic components $i, J_iM \rightarrow f, J_fM$. The effective relaxation is obtained [8] from an average of the relaxation $P_{M\bar{M}}$ for pairs of degenerate components $J_iM \rightarrow J_fM$ and $J_i\bar{M} \rightarrow J_f\bar{M}$, weighted with their relative amplitudes $\langle J_i, M|1,0,J_f,M\rangle$ and $\langle J_i,\bar{M}|1,0,J_f,\bar{M}\rangle$:

$$P(b,v,r) = 1 - \sum_{M,\bar{M}} C_{M\bar{M}}P_{M\bar{M}}(b,v,r), \tag{8}$$

$$\begin{aligned} P_{M\bar{M}}(b,v,r) = \sum_{r'} &\langle i,J_iM,r|S(b,v)|i,J_i\bar{M},r'\rangle \\ &\times\langle f,J_f\bar{M},r'|S^{\dagger}(b,v)|f,J_fM,r\rangle, \end{aligned} \tag{9}$$

where

$$C_{M\bar{M}} = \frac{3}{2J_i+1}\langle J_i,M|1,0,J_f,M\rangle\langle J_i,\bar{M}|1,0,J_f,\bar{M}\rangle$$

is the normalized weight for $P_{M\bar{M}}$ and $\sum_M C_{MM} = 1$.

By use of the transition operator $T = \mathbb{1} - S$, the relaxation function $P(b,v,r)$ can be conveniently split into two "outer" (initial and final) terms and a "middle" term bilinear in T:

$$\begin{aligned} P(b,v,r) = {}& P_{\mathrm{outer},i}(b,v,r) + P_{\mathrm{outer},f}(b,v,r) \\ &+ P_{\mathrm{middle}}(b,v,r), \end{aligned} \tag{10}$$

$$P_{\mathrm{outer},i}(b,v,r) = \frac{1}{2J_i+1}\sum_M \langle i,J_iM,r|T(b,v)|i,J_iM,r\rangle, \tag{11}$$

$$\begin{aligned} &P_{\mathrm{outer},f}(b,v,r) \\ &\quad= \frac{1}{2J_f+1}\sum_M \langle f,J_fM,r|T^{\dagger}(b,v)|f,J_fM,r\rangle, \end{aligned} \tag{12}$$

$$\begin{aligned} &P_{\mathrm{middle}}(b,v,r) \\ &\quad= -\sum_{r',M,\bar{M}} C_{M\bar{M}}\langle i,J_iM,r|T(b,v)|i,J_i\bar{M},r'\rangle \\ &\qquad\times\langle f,J_f\bar{M},r'|T^{\dagger}(b,v)|f,J_fM,r\rangle. \end{aligned} \tag{13}$$

The middle term in Eq. (13), which accounts for correlations between the collisional transitions $i, J_iM, r \rightarrow i, J_i\bar{M}, r'$ and $f, J_fM, r \rightarrow f, J_f\bar{M}, r'$, reduces the contribution to relaxation of the reorienting transitions.

The calculation of P is easily made for weak collisions, i.e., for collisions occurring with such large impact parameters that the intermolecular interaction $V(t)$ can be considered to be a small perturbation on H_0 and the perturbative expansion can be restricted to the lowest order; that for anisotropic interactions is the second. The transition matrix T is then replaced [9] by

$$T_2 = \frac{1}{\hbar^2}\int_{-\infty}^{+\infty} d\omega\, \check{V}(v,b,\omega)\frac{i}{\omega-\omega_0+i\epsilon}\check{V}(v,b,\omega), \tag{14}$$

where $\check{V}(\omega)$ is the Fourier transform of $V(t)$ and $\hbar\omega_0 = \Delta E$ is the total energy transferred in the collision from the internal degrees of the colliders to translation.

While the δ function part of the singular denominator in Eq. (14) contributes to the linewidth, the principal value part contributes to its shift. This second order shift term, not included in the original formulation of the ATC approximation, was considered, for the special case of induction-dispersion forces, by Herman [10] and derived, for the general case of multipolar interactions, by Di Giacomo and Tarrini [9] and later but independently also by Frost [11] and by Boulet *et al.* [12].

By the use of Eq. (14) the real and imaginary parts of the efficiency function P in Eq. (7) can be obtained. We shall denote this approximation by $P^{\mathrm{weak}}(b,v,r)$, in order to emphasize that it is reliable only for weak collisions.

$$\mathrm{Re}P^{\mathbf{weak}}_{\mathbf{outer},a}(b,v,r) = \frac{1}{2\hbar^2}\sum_{a',J'_a,r'} |\langle a, J_a, r\|\check{V}(\omega_{aa'}+\omega_{rr'})\|a', J'_a, r'\rangle|^2, \tag{15}$$

$$\mathrm{Im}P^{\mathbf{weak}}_{\mathbf{outer},a}(b,v,r) = p_a\frac{1}{2\hbar^2}\sum_{a',J'_a,r'} |\langle a, J_a, r\|\tilde{V}(\omega_{aa'}+\omega_{rr'})\|a', J'_a, r'\rangle|^2, \tag{16}$$

$$\mathrm{Re}P^{\mathbf{weak}}_{\mathbf{middle}}(b,v,r) = -\frac{1}{\hbar^2}\sum_{M,\bar{M},r'} C_{M,\bar{M}}\langle i, J_iM, r|\check{V}(\omega_{rr'})|i, J_i\bar{M}, r'\rangle\langle f, J_f\bar{M}, r|\check{V}(\omega_{rr'})|f, J_fM, r'\rangle, \tag{17}$$

$$\mathrm{Im}P^{\mathbf{weak}}_{\mathbf{middle}}(b,v,r) = 0. \tag{18}$$

The label a in Eqs. (15) and (16) can be either i or f, while p_a in Eq. (16) is $+1$ when $a = i$ and -1 when $a = f$. In Eqs. (15)–(17) $\hbar\omega_{\alpha\beta} = E_\beta - E_\alpha$ stands for the energy of the molecular transition $\alpha \to \beta$, while $|\tilde{V}(\omega)|^2$ in Eq. (16) is the Hilbert transform of $|\check{V}(\omega)|^2$:

$$|\tilde{V}(\omega)|^2 = \frac{1}{\pi}\,\mathrm{P}\int_{-\infty}^{\infty} d\omega'\,\frac{|\check{V}(\omega')|^2}{\omega-\omega'}, \tag{19}$$

where P denotes the principal value.

$\hbar(\omega_{aa'}+\omega_{rr'})$ in Eqs. (15) and (16) and $\hbar\omega_{rr'}$ in Eq. (17) are the energy transferred between translation and internal degrees in the collision. P^{weak} decreases rapidly as the transferred energy increases and this provides reliability for the semiclassical approximation. This approximation is inaccurate when the transferred energy is not a small part of the translational energy, but these collisions make a small contribution to P^{weak}. For the same reason, even if the sum in Eqs. (15) and (16) extends over all the transitions $r \to r'$ of the perturber and $a, J_a \to a', J'_a$ of the absorber, vibrational energy changes can usually be excluded because the energy transfer involved is so high that they are negligible.

Explicit expressions can be found in the literature [5, 6, 13] for the various multipolar and polarization interactions of interest in collisions between neutral molecules. For the case of ions one has to also take into account the dipole induced in the perturber by the monopole of the absorber. The dipole-monopole-induced dipole force makes by far the largest contribution to relaxation. So we specialize now to this case:

$$V(t) = -\frac{2\alpha q\boldsymbol{\mu}\cdot\mathbf{R}(t)}{R^6(t)}, \tag{20}$$

where q and $\boldsymbol{\mu}$ are the electric charge and the dipole moment of the absorbing ion, α is the polarizability of the perturber, and $\mathbf{R}(t)$ is the intermolecular distance.

First, we note that $V(t)$ polarizes the perturber without inducing transitions in its internal state r. If we assume α independent of r, $P(b,v,r) \simeq P(b,v)$, and Eq. (7) becomes

$$w + is = \left\langle 2\pi nv\int_0^{\infty} bdb\,P(b,v)\right\rangle_v . \tag{21}$$

Moreover in Eqs. (15)–(17) $r' = r$. Hence

$$\mathrm{Re}P^{\mathbf{weak}}_{\mathbf{outer},a}(b,v) = \frac{1}{2\hbar^2}\sum_{a',J'_a} |\langle a, J_a\|\check{V}(\omega_{aa'})\|a', J'_a\rangle|^2, \tag{22}$$

$$\mathrm{Im}P^{\mathbf{weak}}_{\mathbf{outer},a}(b,v) = p_a\frac{1}{2\hbar^2}\sum_{a',J'_a} |\langle a, J_a\|\tilde{V}(\omega_{aa'})\|a', J'_a\rangle|^2, \tag{23}$$

$$\mathrm{Re}P^{\mathbf{weak}}_{\mathbf{middle}}(b,v) = -\frac{1}{\hbar^2}\sum_{M,\bar{M}} C_{M,\bar{M}}\langle i, J_iM|\check{V}(0)|i, J_i\bar{M}\rangle \times\langle f, J_f\bar{M}|\check{V}(0)|f, J_fM, r'\rangle. \tag{24}$$

The integration along the collisional trajectory can be performed in closed form if one uses the approximation of a straight line path. This is carried out in the Appendix, following the same scheme used in Refs. [6, 13] for different interactions.

For the real part of $P^{\mathrm{weak}}_{\mathrm{outer}}(b,v)$ we obtain

$$\mathrm{Re}P^{\mathbf{weak}}_{\mathbf{outer},a}(b,v) = \frac{A}{v^2b^8}\sum_{a'J'_a} |\langle a, J_a\|\mu\|a', J'_a\rangle|^2 g(k_{aa'}), \tag{25}$$

where

$$A = \frac{3}{32}\left(\frac{\pi\alpha q\mu}{\hbar}\right)^2, \tag{26}$$

$$k_{aa'} = \omega_{aa'}b/v, \tag{27}$$

and the broadening resonance function $g(k)$, plotted in Fig. 1, is

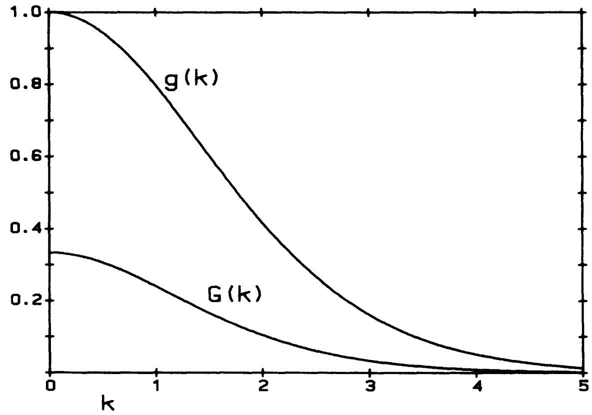

FIG. 1. Shape of the broadening resonance functions $g(k)$ and $G(k)$ describing, for the case of dipole-monopole-induced dipole interaction, the dependence of the line broadening real part of the semiclassical relaxation efficiency function on the product of the duration of the collision and the energy transferred from translation to the internal degrees of the absorbing molecule; see Eq. (27). Both g and G are even functions of k.

$$g(k) = e^{-2|k|}(9 + 18|k| + 16k^2 + 8|k|^3 + 2k^4)/9. \qquad (28)$$

$\langle a, J_a \| \mu \| a', J'_a \rangle$ in Eq. (25) is the reduced dipole moment matrix element for the transition $a, J_a \to a', J'_a$.

For $P^{\text{weak}}_{\text{middle}}(b, v)$ we obtain

$$P^{\text{weak}}_{\text{middle}}(b, v) = \frac{2A}{v^2 b^8} \langle i, J_i \| \mu \| i, J_i \rangle \langle f, J_f \| \mu \| f, J_f \rangle \times (-1)^{J_i + J_f + 1} (2J_i + 1)^{1/2} (2J_f + 1)^{1/2} W \times (J_i, J_f, J_i, J_f; 1, 1), \qquad (29)$$

where $W(J_i, J_f, J_i, J_f; 1, 1)$ is a Racah coefficient due [8] to the sum over the degenerate magnetic quantum numbers M and $\bar{M}$ in Eq. (24). This second order middle term is present only for ions that, as the symmetric tops, have a permanent dipole moment component reoriented by collisions. For a linear absorber as HCO^+: $\langle a, J_a \| \mu \| a, J_a \rangle = 0$ and the middle term vanishes.

For the imaginary part of $P(b, v)$ we obtain

$$\text{Im} P^{\text{weak}}_{\text{outer},a}(b, v) = \frac{A}{v^2 b^8} \sum_{a' J'_a} |\langle a, J_a \| \mu \| a', J'_a \rangle|^2 \tilde{g}(k_{aa'}), \qquad (30)$$

where the shifting resonance function $\tilde{g}$ is the Hilbert transform of g and is plotted in Fig. 2. Its behavior for very small or large values of k is $\tilde{g}(k) \simeq (15k - 2k^3 + \cdots)/9\pi$ when $|k| \ll 1$, while $\tilde{g}(k) \simeq (35/k + 189/k^3 + 891/k^5 + \cdots)/9\pi$ when $|k| \gg 1$.

Equations (25)–(30) give an explicit expression of the efficiency function P^{weak}, reliable for the case of weak collisions occurring at large values of the impact parameter b. This expression is divergent for $b \to 0$. However, the case of strong collisions is easily evaluated, because all coherence is lost and

$$P^{\text{strong}} = 1. \qquad (31)$$

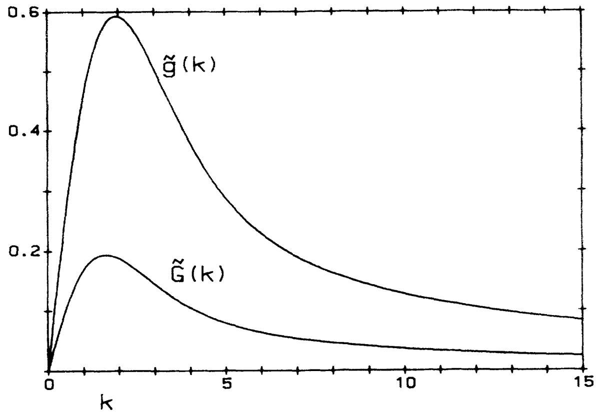

FIG. 2. Shape of the shifting resonance functions $\tilde{g}$ and $\tilde{G}$. They are, respectively, the Hilbert transform of g and G and describe the dependence of the line shifting imaginary part of the semiclassical relaxation efficiency function on the product of the duration of the collision and the energy transferred from translation to the internal degrees of the absorbing molecule. Both $\tilde{g}$ and $\tilde{G}$ are odd functions of k.

For the intermediate b range, Anderson proposed [5] three different solutions, while other solutions have been proposed [14–16], as discussed in Ref. [17]. However, the choice of one or another of these approximations produces only changes of 10–20 % in the final results for both width and shift. We use the second solution proposed by Anderson, as modified in Ref. [16] in order to take into account also the imaginary part of P. It consists in an extrapolation of the known limiting strong and weak cases. P^{weak} is used as long as $|P^{\text{weak}}(b, v)| \leq 1$. When, on reducing b, $|P^{\text{weak}}(b, v)|$ reaches 1, a cutoff impact parameter b_0 is introduced and P^{strong} is used for $b > b_0$.

Within this approximation, the integration over b in Eq. (21) can be performed explicitly yielding

$$w + is = n \Big\langle v\sigma(v) \Big\rangle_v, \qquad (32)$$

$$\text{Re}\sigma(v) = \pi b_0^2 \Bigg[1 + \frac{A}{v^2 b_0^8} \Bigg(\sum_{i', J'_i} |\langle i, J_i \| \mu \| i', J'_i \rangle|^2 G(k_{ii'}) + \sum_{f', J'_f} |\langle f, J_f \| \mu \| f', J'_f \rangle|^2 G(k_{ff'}) + \frac{2}{3} \langle i, J_i \| \mu \| i, J_i \rangle \langle f, J_f \| \mu \| f, J_f \rangle (-1)^{J_i + J_f + 1} (2J_i + 1)^{1/2} (2J_f + 1)^{1/2} \times W(J_i, J_f, J_i, J_h; 1, 1) \Bigg) \Bigg], \qquad (33)$$

and

$$\text{Im}\sigma(v) = \pi \frac{A}{v^2 b_0^6} \Bigg(\sum_{i', J'_i} |\langle i, J_i \| \mu \| i', J'_i \rangle|^2 \tilde{G}(k_{ii'}) - \sum_{f', J'_f} |\langle f, J_f \| \mu \| f', J'_f \rangle|^2 \tilde{G}(k_{ff'}) \Bigg). \qquad (34)$$

In Eqs. (33) and (34), $k_{aa'} = \omega_{aa'} b_0 / v$. The resonance function $G(k) = e^{-2|k|}(3 + 6|k| + 5k^2 + 12|k|^3)/9$ is plotted in Fig. 1, while its Hilbert transform $\tilde{G}$ is plotted in Fig. 2. When $|k| \ll 1$, $\tilde{G}(k) \simeq (6k - 4k^3/3 + \cdots)/9\pi$, while $\tilde{G}(k) \simeq (10/k + 21/k^3 + 182/k^5 + \cdots)/9\pi$ when $|k| \gg 1$.

III. EXPERIMENT

The frequency-modulated (FM) mm–sub-mm source employed in this work has been described in detail in a previous paper [18]. A crystal harmonic generator is driven by a klystron, which is stabilized with respect to a frequency synthesizer by means of two phase-lock loops. The use of a wide-band klystron synchronizer allows two scanning schemes, either sweeping the frequency synthesizer at the beginning of the synchronization chain, or sweeping the sine-wave modulated reference signal of the klystron synchronizer.

The third harmonic of a 30V12 Oki klystron was used for recording the $J = 1 \leftarrow 0$ line, and the third and the sixth harmonics of a VRE2103B-11 Varian klystron were used for the $J = 2 \leftarrow 1$ and $J = 4 \leftarrow 3$ lines. Cutoff filters were employed to suppress lower harmonics than that of interest. Harmonics of higher order could usually be minimized by adjusting the frequency multiplier geometry, but in the case of the $J = 1 \leftarrow 0$ line we were not able to completely suppress the $J = 2 \leftarrow 1$ line; this reduced the accuracy of the determination of the frequency shift, as explained below.

A homemade Schottky barrier detector was used for the line at 89.2 GHz, and the higher frequency lines were detected by means of a liquid-He-cooled silicon bolometer. Lock-in detection at 2 f and computer-controlled data acquisition were employed.

The absorption cell is a 4-m-long Pyrex tube, 9 cm in diameter, wound with a solenoid, which provides a longitudinal magnetic field of up to 200 G, and a plastic pipe for cooling the cell by flowing liquid nitrogen. The cell is equipped at the ends with two cylindrical electrodes 40 cm in length, and in the middle with a ring-shaped electrode 5 mm wide, which acts as the cathode. In this arrangement there are two half-cells with opposite polarity and this has the effect of making the contribution from the Doppler shift (due to ion drift velocity) symmetrical. The negative glow regions of the two discharges, where the positive ions are produced, fill the length of the cell. Because of the small surface of the cathode, the dc discharge current does not increase very much with increasing buffer gas pressure. This prevents switching from an anomalous glow discharge, characterized by low current and high voltage, to a normal glow discharge with high current and low voltage.

The vacuum system consists of a diffusion pump backed by a mechanical pump. This allows a fast flow rate, but prevents high pressure measurements ($p > 35$ mTorr) due to the failure of the diffusion pump in maintaining a constant flow through the cell. Reduction of the pump throughput to raise the pressure in the cell above this limit gives poorer spectra. The pressure is monitored by a MKS Instruments capacitance manometer with a resolution of 0.1 mTorr.

An input flow of a 1:1 mixture of CO and H_2 was set to give a constant pressure in the cell (in the 0.5–2 mTorr range) and the discharge voltage was set to the maximum value allowed by the discharge power supply (3.8 kV), then an Ar flow was introduced into the cell. Even with a discharge current less than 1 mA, at Ar pressures of a few mTorr, HCO^+ could be detected in the liquid-nitrogen-cooled anomalous glow discharge. The total pressure was adjusted by changing the buffer gas input rate. The discharge current ranged from 1 to 20 mA for Ar pressures between 2 and 35 mTorr; the discharge voltage was almost constant after dropping from 3.8 to 3.4 kV for currents higher than 5 mA: under these discharge conditions the HCO^+ signal was a maximum at each pressure. Changes in the discharge current of 10 mA induce variations in the total pressure of only a few tenths of a mTorr. Measurements at constant discharge current, instead of constant discharge voltage, showed no significant change in the broadening parameters. In addition, measurements under such conditions can be carried out only over a limited range of pressure, since at higher pressures the HCO^+ line becomes very weak.

A critical operating condition is the cell cooling. If the plastic tube wound around the cell is not completely full of liquid nitrogen, the wall temperature tends to rise and the linewidth is immediately affected. Other conditions were tested, such as different pressures of the CO-H_2 mixture or different pumping speeds, but the collisional parameters were not affected significantly. Thus, statistical fluctuations or uncontrolled systematic effects (often related to background problems in line profile analysis) seem to dominate the uncertainties. Measurements for lines of different J were carried out under similar conditions. If systematic errors related to the discharge parameters are present, they should affect the results for different J's in the same way, thus preserving the accuracy in the trend of the collisional parameters as a function of the rotational quantum number.

IV. DATA ANALYSIS

To recover collisional linewidth from the recorded spectra, we employed the Pickett's convolution method [19] also described in Ref. [20]. In this procedure, it is important to have a good quality reference spectrum recorded at low pressure and with the base-line removed. The same modulation scheme and modulation depth of the reference have to be employed for all the spectra. All the pressure independent effects, such as Doppler broadening and spectral modulation, are contained in the reference spectrum. This is then convoluted with a Lorentz function to account for the collisional contribution to the line shape of the higher pressure spectra. The experimental profiles were fitted in the least-squares sense to this convoluted spectrum with the inclusion of base-line corrections.

Because of the poor signal-to-noise ratio in the low pressure spectra, reference spectra were recorded at an Ar pressure of $\simeq 7$ mTorr. The base-line was removed by subtraction of a polynomial curve fitted to the points at both sides of the spectral feature. The fitted Lorentzian widths are half-widths at half maximum (HWHM) and are relative to the pressure difference (in the range 0–30 mTorr) between the broadened and the reference spectrum.

For each line 5–7 series of measurements at 7–9 increasing values of Ar pressure were carried out. The linear fits of the full set of Lorentzian linewidths for each rotational transition are reported in Fig. 3. The data were weighted by the squared reciprocal of the uncertainties from the profile fits.

Another method to analyze the line shape is to fit the spectrum to a profile which explicitly accounts for frequency modulation. The implementation of such a method for second harmonic FM detection of Doppler and pressure broadened lines has been previously described [18]. The experimental 2 f signal is fitted to the computed second Fourier component of a modulated Voigt profile. The asymmetry of the spectral lines due to the frequency dependence of the effective path length in the free space absorption cell is accounted for by means of a suitable distortion term. In this way the apparent instrumental line shift can be allowed for, thus giving

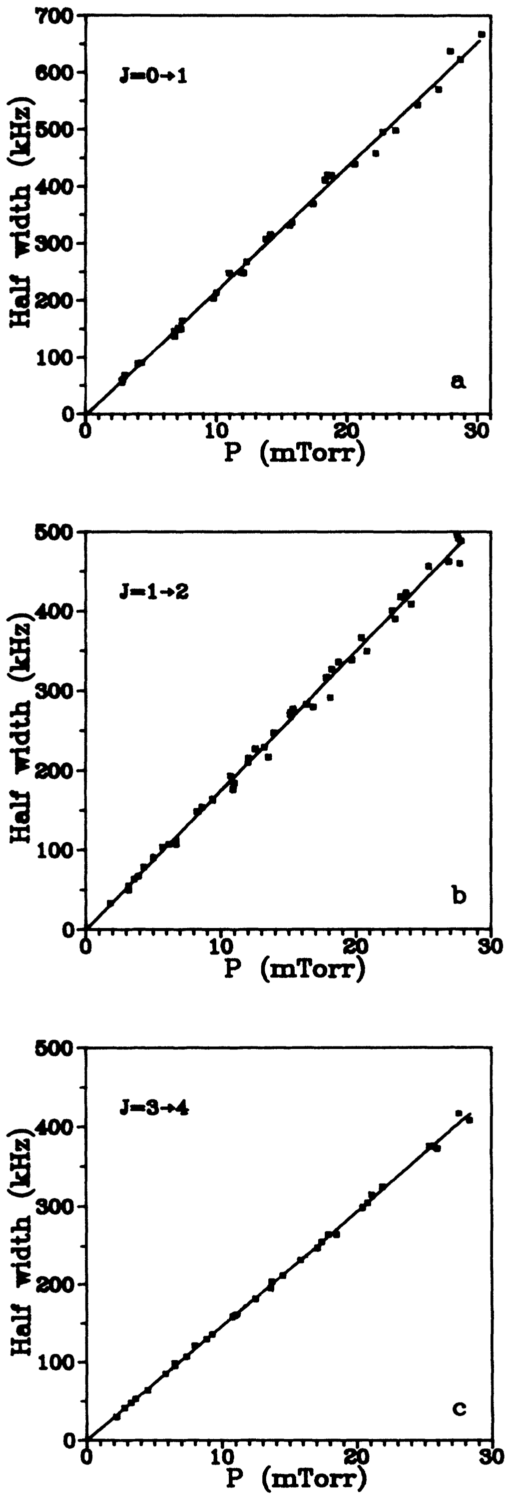

FIG. 3. Plots of Lorentzian linewidth (HWHM) vs pressure for HCO$^+$ lines broadened by Ar. The straight lines are the least-squares fits of the data.

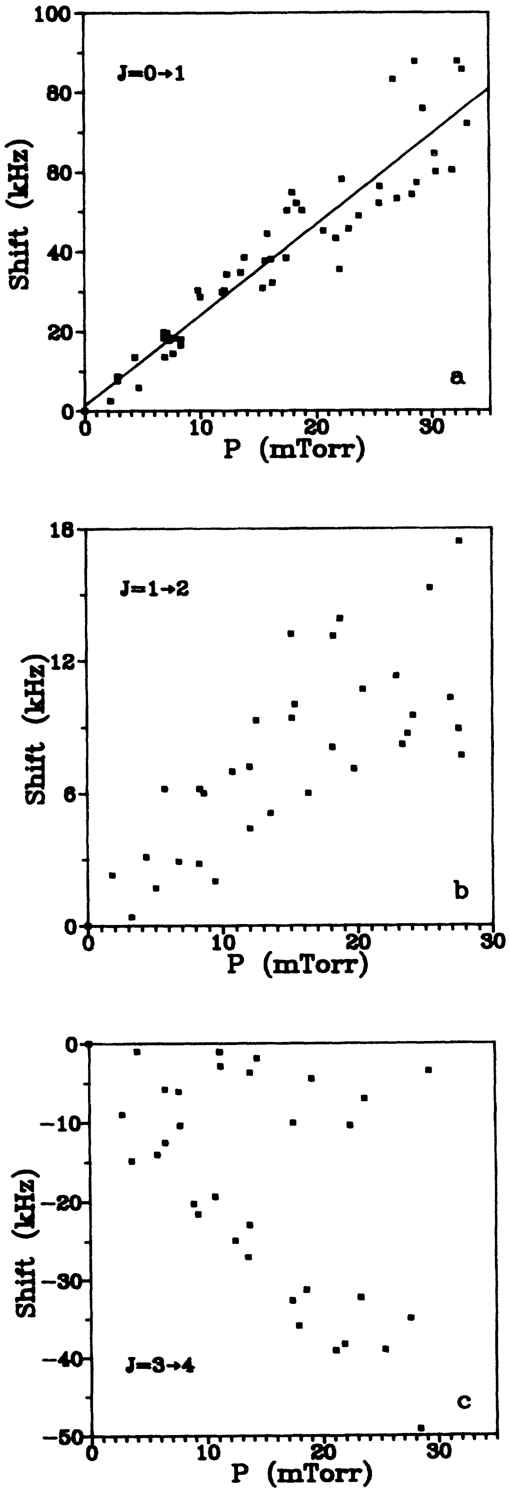

FIG. 4. Plots of frequency shift vs pressure for HCO$^+$ lines perturbed by Ar. The straight line is the least-squares fit.

a better evaluation of the pressure-shift. We have also adopted this procedure in studying the frequency shift induced by collisions.

Pressure-shift measurements are more critical than pressure-broadening measurements, mainly because frequency shifts are small and compete with instrumental shifts. The latter can be corrected for by adjusting the standing wave pattern in the cell, so affecting the asymmetry in the second harmonic line profile, which is responsible for the apparent line shift. But the effective path length in the cell also depends on the plasma conditions, which change during the experiment particularly at higher pressures. It is therefore difficult to control line asymmetry sources and we were unable to record pairs of spectra at the same pressure with opposite asymmetry, a procedure which allowed us to properly account for instrumental line shift for carbonyl sulfide (OCS) rotational transitions [18]. For the $J = 1 \leftarrow 0$ line the presence of a sixth-harmonic small signal due to the $J = 2 \leftarrow 1$ transition contributed to the line shape asymmetry. The competition of the factors made it difficult to correct for the instrumental line shift and this is reflected in the dispersion of the pressure-shift data, as shown in Fig. 4(a). For the $J = 2 \leftarrow 1$ and $J = 4 \leftarrow 3$ transitions the pressure-shift parameters are predicted to be smaller than that of the $J = 1 \leftarrow 0$. This fact, in combination with the problems discussed above, allowed us to determine only the sign of the pressure-shift. Figures 4(b) and 4(c) show that, despite the scatter of the data, there is a definite positive trend of line shift versus pressure for the $J = 2 \leftarrow 1$ transition, and a definite negative trend for the $J = 4 \leftarrow 3$ transition. The line shift data shown in Fig. 4 are the result of several series of measurements at increasing pressure; the center frequency of the lowest-pressure spectrum in each series was assumed as a reference for determining the frequency-shift of the higher pressure spectra.

Finally, we examined the sources of broadening at very low pressures in an attempt to determine the ion temperature from the Doppler width. For this purpose the line profile was fitted to a modulated Voigt profile, as explained above. The $J = 4 \leftarrow 3$ is a good test transition, since the Doppler width at 77 K is comparable to the Lorentz width in the medium pressure range. Because of the correlation between the two width parameters in the line profile fit, we performed a global fit in which all the spectra of a complete sequence recorded with increasing Ar pressure (3–20 mTorr) were simultaneously fitted to the line profile model with the linewidth parametrized by only three fitting parameters (the Doppler width, the pressure-broadening coefficient, and the residual Lorentz width at zero Ar pressure).

Three series at different CO-H_2 mixture pressures (0.5–2 mTorr) were examined. The fitted pressure-broadening parameter agreed with the value obtained previously; the average Doppler width was 172(2) kHz, corresponding to a 53 K temperature. This low value suggests that the Voigt profile might be not fully adequate in describing the line profile. In fact, since the Voigt profile neglects the correlation between Doppler and collisional broadening, more complicated line shapes were proposed [21, 22]. An attempt to fit the experimental profiles to such line shapes, fixing the Doppler width at the value corresponding to 77 K, led to a better residual pattern. A more detailed investigation of this effect could give information on the diffusion coefficient of HCO^+ in argon, but this is not the aim of the present paper. We conclude by pointing out that the use of these more sophisticated line shapes affects negligibly the collisional broadening and shift parameters, while leading to rather different results for the residual Lorentzian width at zero Ar pressure, which accounts for collisions with CO and H_2.

V. RESULTS AND DISCUSSION

Measured and calculated values for collisional line broadening and shift are reported in Table I. The experimental errors are 1σ statistical uncertainties from the linear fit. They overestimate the accuracy of the pressure broadening parameters. From an analysis of different series of measurements this can be estimated to be about 5%. For two lines we could evaluate only the sign of the pressure shift. The 3σ uncertainty for the shift of the $J = 1 \leftarrow 0$ transition is 8% of the parameter value and

TABLE I. Measured and calculated broadening and shift parameters of HCO^+ rotational lines perturbed by argon at 77 K.

Line J''	Frequency (MHz)	Broadening (MHz/Torr)		Shift (MHz/Torr)	
		Expt.[a]	Theor.	Expt.[a]	Theor.
0	89 188.53	21.49 (21)	21.02	+2.27 (6)	+2.91
1	178 375.06	17.51 (19)	17.22	+	+0.85
2	267 557.619[b]		13.17		+0.01
3	356 734.25	14.56 (7)	10.25	−	−0.28
4	445 902.996[b]		8.15		−0.40
5	535 061.711[b]		6.58		−0.48

[a] The standard errors from the linear fit in units of the last quoted digit are reported in parentheses. They overestimate the accuracy of the pressure broadening parameters. From an analysis of different series of measurements this can be estimated to be about 5%.

[b] G. A. Blake, K. B. Laughlin, R. C. Cohen, K. L. Busarow, and R. J. Saykally, Astrophys. J. **316**, L45 (1987).

this seems a reasonable accuracy for this type of measurement.

The theoretical values were calculated using the theory described in Sec. II and assuming a temperature of 77 K. We used a value of 3.91 D [23] for the dipole of HCO^+ and 1.64×10^{-24} cm^3 for the argon polarizability [24].

The reliability of the approximations involved in the theory is better when the broadening cross section $\sigma = w/nv$ is much larger than the kinetic cross section. In our case the radius of the broadening cross section is of about 1 nm, hence this condition is well satisfied. In order to evaluate the error due to the use of straight line collisional trajectories, we must compare the average kinetic energy to the energy of the monopole-monopole-induced dipole interaction, at an ion-perturber distance equal to the average cutoff radius. In our case the interaction energy is about 10% of the translational energy, so that some improvement of the calculated values could be found by a numerical integration of the translational motion in Eqs. (22)–(24). This work is in progress. However, this kind of error is of the same order as those due to the other approximations used by the theory: semiclassical approximation and second order scattering matrix.

On the whole, in view of the experimental errors and of the approximate character of the theory, the agreement between measurements and calculations is satisfactory. There is a good agreement for the magnitude of the two measured parameters, the decrease with J of the broadening, and the change in sign of the shift parameters.

The largest difference (30%) is found for the broadening of the $J = 4 \leftarrow 3$ transition. This seems to indicate that the theory overestimates the decrease of the broadening parameter for increasing J values, a feature already noted for the ATC calculations of the broadening of the lines of neutral molecules [20, 25]. The J dependence of the broadening parameter is essentially due to the energy differences between the initial and final states of the line J_i, J_f and the near-lying states $J_i \pm 1$, $J_f \pm 1$. This affects $\omega_{aa'}$ in Eq. (22), $k_{aa'}$ in Eq. (25), and $k_{ii'}$ and $k_{ff'}$ in Eq. (33). Hence, the discrepancy could be due to a too rapid decrease, for large values of k, of the broadening resonance function $g(k)$ defined by Eq. (28). However, a reliable analysis of this minor discrepancy would be possible only with a more extended study, including also other J values.

For the moment, we restrict ourselves to conclude that the experimental data confirm what we have shown in Sec. II on the interactions affecting the shape of the lines of molecular ions by collisions with neutral perturbers. The effect of the ionic monopole is restricted to that of inducing on the neutral perturbers a polarization that can cause relaxation by interaction with the permanent moments of the absorbing ion, with the exclusion of the monopole. Among these, the dipole-monopole-induced dipole interaction makes by far the largest relaxation effect.

Hence, the theoretical treatment that we developed in this paper in the frame of the ATC approximation can have a general use for the calculation of the broadening and shift of the lines of molecular ions by collisions with neutral perturbers. If the perturber is not a noble gas atom, but a molecule with permanent multipolar moments, the interactions between the permanent moments of the absorber (with the exclusion of the monopole) and of the perturber must be also taken into account, following the methods used for a long time for neutral absorbers.

ACKNOWLEDGMENTS

We thank Professor David Lister for his reading of the manuscript. This work was supported by MURST and CNR.

APPENDIX

In a reference system with the y axis in the direction of the straight line classical trajectory and the z axis in the direction joining the centers of the two molecules at the moment $t = 0$ of closest approach, we have $R_x = 0$, $R_y = vt$, $R_z = b$, and $R = \sqrt{b^2 + v^2t^2}$. Hence

$$\begin{aligned}\check{V}(\omega) &= \int_{-\infty}^{+\infty} dt\, e^{i\omega t} \frac{-2\alpha q \boldsymbol{\mu} \cdot \mathbf{R}(t)}{R^6(t)} \\ &= -2\alpha q \left(\mu_z \int_{-\infty}^{+\infty} dt\, \frac{e^{i\omega t} b}{(b^2 + v^2t^2)^3} \right. \\ &\quad \left. + \mu_y \int_{-\infty}^{+\infty} dt\, \frac{e^{i\omega t} vt}{(b^2 + v^2t^2)^3} \right) \\ &= -2\alpha q (\mu_z I_z + \mu_y I_y). \end{aligned} \tag{A1}$$

The two integrals I_z and I_y can be calculated by contour integration:

$$I_z = \int_{-\infty}^{+\infty} dt\, \frac{e^{i\omega t} b}{(b^2 + v^2t^2)^3} = \frac{\pi}{8vb^4} e^{-|k|}(3 + 3|k| + k^2), \tag{A2}$$

$$I_y = \int_{-\infty}^{+\infty} dt\, \frac{e^{i\omega t} vt}{(b^2 + v^2t^2)^3} = \frac{i\pi}{8vb^4} e^{-|k|}(k + k|k|), \tag{A3}$$

where $k = \omega b/v$.

Now, in order to evaluate $\text{Re}P(b, v)_{\text{outer},a}$ in Eq. (22), we must calculate $|\check{V}(\omega)|^2$ and perform an average on the direction of $\boldsymbol{\mu}$. Since the average of μ_z^2 and μ_y^2 is $\mu^2/3$, while the average of $\mu_z\mu_y$ is 0, from Eq. (A1) we have

$$\begin{aligned} &|\langle a, J_a \| \check{V}(\omega_{aa'}) \| a', J'_a \rangle|^2 \\ &\quad = |\langle a, J_a \| \mu \| a', J'_a \rangle|^2 \, 4\alpha^2 q^2 \frac{\mu^2}{3} (I_z^2 - I_y^2) \\ &\quad = |\langle a, J_a \| \mu \| a', J'_a \rangle|^2 \, \frac{3\pi^2 \alpha^2 q^2 \mu^2}{16 v^2 b^8} g(k), \end{aligned} \tag{A4}$$

where the resonance function $g(k)$ is given by Eq. (28). The use of Eq. (A4) in Eq. (22) yields Eq. (25). The integration that yields Eq. (29) from Eq. (24) is completely analogous, but for the Racah coefficient due [8] to the sum over the degenerate magnetic quantum number. We note that the average on the direction of the dipole moment could also be performed by the use of spherical harmonics, as in Refs. [6, 13] for different interactions. We preferred the present scheme for the sake of simplicity.

[1] E. Herbst and W. Klemperer, Astrophys. J. **188**, 255 (1974).
[2] B. E. Turner, Astrophys. J. **193**, L83 (1974).
[3] R. C. Woods, in *Molecular Ions: Spectroscopy, Structure, and Chemistry*, edited by T. A. Miller and V. E. Bondybey (North-Holland, Amsterdam, 1983), and references therein.
[4] T. G. Anderson, C. S. Gudeman, T. A. Dixon, and R. C. Woods, J. Chem. Phys. **72**, 1332 (1980); C. S. Gudeman, Ph.D. thesis, University of Wisconsin, Madison, 1982.
[5] P. W. Anderson, Phys. Rev. **76**, 647 (1949).
[6] C. T. Tsao and I. Curnutte, J. Quant. Spectrosc. Radiat. Transfer **2**, 41 (1962).
[7] M. Baranger, Phys. Rev. **111**, 481 (1958); U. Fano, *ibid.* **131**, 259 (1963); A. Di Giacomo, Nuovo Cimento **34**, 473 (1964); A. Ben-Reuven, Phys. Rev. **141**, 34 (1966).
[8] G. Buffa, A. Di Lieto, P. Minguzzi, O. Tarrini, and M. Tonelli, Phys. Rev. A **34**, 1065 (1986).
[9] A. Di Giacomo and O. Tarrini, Nuovo Cimento B **62**, 1 (1969); **68**, 165 (1970).
[10] R. M. Herman, Phys. Rev. **132**, 262 (1963).
[11] B. S. Frost, J. Phys. B **9**, 1001 (1976).
[12] C. Boulet, D. Robert, and L. Galatry, J. Chem. Phys. **65**, 5302 (1976).
[13] Krishnaji and S. L. Srivastava, J. Chem. Phys. **41**, 2266 (1964); **42**, 1546 (1965).
[14] J. S. Murphy and J. E. Boggs, J. Chem. Phys. **47**, 691 (1967).
[15] D. Robert and J. Bonamy, J. Phys. (Paris) **40**, 923 (1979).
[16] G. Baldacchini, S. Marchetti, V. Montelatici, G. Buffa, and O. Tarrini, J. Chem. Phys. **76**, 5271 (1982).
[17] G. Buffa and O. Tarrini, Appl. Opt. **28**, 1800 (1989).
[18] G. Cazzoli and L. Dore, J. Mol. Spectrosc. **141**, 49 (1990).
[19] H. M. Pickett, Appl. Opt. **19**, 2745 (1980).
[20] L. Dore, G. Cazzoli, M. E. Charro, C. Degli Esposti, G. Buffa, and O. Tarrini, J. Mol. Spectrosc. **160**, 345, (1993).
[21] R. Galatry, Phys. Rev. **122**, 1218 (1961).
[22] S. G. Rautian and I. I. Sobleman, Usp. Fiz. Nauk **90**, 209 (1966) [Sov. Phys. Usp. **9**, 701 (1967)].
[23] P. Botschwina, in *Ion and Cluster Ion Spectroscopy and Structure*, edited by J. P. Maier (Elsevier, Amsterdam, 1989).
[24] C. G. Gray and K. E. Gubbins, *Theory of Molecular Fluids* (Clarendon Press, Oxford, 1984), Vol. 1.
[25] G. Baldacchini, G. Buffa, and O. Tarrini, Nuovo Cimento D **13**, 719 (1991); G. Buffa, O. Tarrini, P. De Natale, M. Inguscio, F. S. Pavone, M. Prevedelli, K. M. Evenson, L. R. Zink, and G. W. Schwaab, Phys. Rev. A **45**, 6443 (1992); V. N. Markov, A. S. Pine, G. Buffa, and O. Tarrini, J. Quant. Spectrosc. Radiat. Transfer **50**, 167 (1993).